ISSN 0036-0236, Russian Journal of Inorganic Chemistry, 2017, Vol. 62, No. 9, pp. 1197–1201. © Pleiades Publishing, Ltd., 2017.
Original Russian Text © S.I. Bezzubov, A.A. Bilyalova, I.S. Zharinova, M.A. Lavrova, Yu.M. Kiselev, V.D. Dolzhenko, 2017, published in Zhurnal Neorganicheskoi Khimii, 2017, Vol. 62, No. 9, pp. 1205–1209.

PHYSICAL METHODS OF INVESTIGATION

Synthesis, Structure, and Optical Properties of Lanthanum(III), Cerium(III), Praseodymium(III), and Nickel(II) Heterometallic Complexes with Glycine

S. I. Bezzubov[a, *], A. A. Bilyalova[b], I. S. Zharinova[b], M. A. Lavrova[b], Yu. M. Kiselev[b], and V. D. Dolzhenko[b]

[a] *Kurnakov Institute of General and Inorganic Chemistry, Russian Academy of Sciences, Moscow, 119991 Russia*
[b] *Department of Chemistry, Moscow State University, Moscow, 119991 Russia*
**e-mail: bezzubov@igic.ras.ru*

Received October 12, 2016

Abstract—New cluster complexes of lanthanides(III) and nickel(II) $[Ln\{Ni(Gly)_2\}_6]^{3+}[Ln(NO_3)_6]^{3-}$ have been synthesized, where Ln = La (**I**), Ce (**II**), and Pr (**III**); and Gly is glycinate. The structures of compounds **I**–**III** are determined by X-ray diffraction. The icosahedral cavity in the complex cation, where the lanthanide ion resides, has a fixed size independent of the nature of the central Ln(III) ion. In the complex anion, on the contrary, the Ln–O distances naturally decrease from La(III) to Pr(III). The optical properties of cation–anion complexes **I**–**III** are studied. Based on the assignment in the electronic absorption spectra of the complexes, it is shown that the absorption bands are caused by *d*–*d* electronic transitions.

DOI: 10.1134/S0036023617090030

Polynuclear 3*d*–4*f* cluster complexes, which self-organize from as simple building blocks as trivalent lanthanide ions and *d*-metal salts with amino acids, attract attention due to their potential use as molecular magnets [1]. To date, these complexes with a large number of natural and synthetic amino acids have been investigated [2]. Earlier, we studied the $LnNi_6$ octahedral clusters based on L-alanine and proposed an efficient method to isolate these complexes into the solid phase by forming cation-anionic compound $[Ln\{Ni(Ala)_2\}_6]^{3+}[Ln(NO_3)_3(OH)_3(H_2O)]^{3-}$, where Ala is L-alaninate [3]. In the present work, we have investigated the structure and optical properties of the related complexes with the composition of $[Ln\{Ni(Gly)_2\}_6]^{3+}[Ln(NO_3)_6]^{3-}$ for La(III), Ce(III), and Pr(III) using glycine as an amino acid.

EXPERIMENTAL

Commercially available reagents of pure for analysis grade or higher purity grade were used in the work without further purification. Lanthanide nitrates were prepared by dissolving the corresponding oxides in concentrated nitric acid followed by evaporation of the solutions to dryness. Nickel(II) glycinate was synthesized according to [4].

Complexes **I**–**III** were prepared in two stages: (1) synthesis of a complex cation in an alcoholic solution; and (2) precipitation of the target cation–anionic compounds. In detail, the procedure is described below for compound **I**.

Dodecakis(μ_2-glycinato-1:2κ^2O:N,O)lanthanum(III)-hexanickel(II) hexakis-(nitrato-κ^2O,O')lanthanate(III) $[La\{Ni(Gly)_2\}_6]^{3+}[La(NO_3)_6]^{3-}$ (I). NaOH (0.3 mmol) was added on stirring to a solution containing $Ni(NO_3)_2 \cdot 6H_2O$ (97 mg, 0.33 mmol), $La(NO_3)_3 \cdot 6H_2O$ (24 mg, 0.055 mmol), and glycine (50 mg, 0.67 mmol) in H_2O (10 mL). The resulting solution was stirred at 80°C for 1 h. The green solution became violet. EtOH (10 mL) was added to the solution. After 10–15 min, a coarse-crystalline violet precipitate was observed to form. After 2–3 h, the crystals were separated, dried, and ground to a fine powder. The powder was washed with a small amount of alcohol followed by diethyl ether and dried at 50°C in vacuum for 10 h. Yield, 95%.

Dodecakis-(μ_2-glycinato-1:2κ^2O:N,O)cerium(III)-hexanickel(II) hexakis-(nitrato-κ^2O,O')cerate(III) $[Ce\{Ni(Gly)_2\}_6]^{3+}[Ce(NO_3)_6]^{3-}$ (II). Violet powder. Yield, 96%.

Dodecakis-(μ_2-glycinato-1:2κ^2O:N,O)praseodymium(III)hexanickel(II) hexakis-(nitrato-κ^2O,O')praseodymate(III) $[Pr\{Ni(Gly)_2\}_6]^{3+}[Pr(NO_3)_6]^{3-}$ (II). Violet powder. Yield, 90%.

The structures and compositions of complexes **I**–**III** were determined by a combination of the single-crys-

Table 1. Crystallographic data, details of data collection, and characteristics of data refinement for complexes **I**–**III**

	I	**II**	**III**
Molecular formula	$C_{24}H_{48}La_2N_{18}Ni_6O_{42}$	$C_{24}H_{48}Ce_2N_{18}Ni_6O_{42}$	$C_{24}H_{48}N_{18}Ni_6O_{42}Pr_2$
FW	1890.88	1893.30	1894.88
Crystal size, mm	0.30 × 0.10 × 0.10	0.40 × 0.40 × 0.40	0.40 × 0.40 × 0.40
Syngony		Trigonal	
Space group	$R\bar{3}c$	$R\bar{3}c$	$R\bar{3}c$
a, Å	15.7239(18)	15.7255(16)	15.7506(9)
c, Å	37.094(9)	37.063(7)	37.050(4)
V, Å^3	7943(2)	7937(2)	7960.1(11)
Z	6	6	6
ρ_{calc}, g/cm^3	2.372	2.377	2.372
μ, mm^{-1}	3.796	3.904	4.013
F(000)	5616	5628	5640
θ range, deg	2.59–30.00	2.59–30.00	2.59–30.00
h, k, l index intervals	$-21 \le h \le 22$, $-22 \le k \le 22$, $-52 \le l \le 51$	$-22 \le h \le 22$, $-22 \le k \le 22$, $-52 \le l \le 52$	$-13 \le h \le 20$, $-22 \le k \le 14$, $-34 \le l \le 50$
Number of collected reflections	30327	29550	10015
Number of unique reflections	2586	2583	2574
Data completeness for θ, %	100	100	99.2
Number of variables	140	140	140
Goodness-on-fit on F^2	1.035	1.064	1.052
R_1 for $I > 2\sigma(I)$	0.0177	0.0223	0.0224
wR_2 (all data)	0.0395	0.0573	0.0565
$\Delta\rho_{max}/\Delta\rho_{min}$, e/Å^3	0.484/–0.443	0.609/–0.855	0.635/–0.792

tal X-ray diffraction and X-ray powder diffraction methods. In X-ray powder diffraction patterns, all reflections were indexed in space group $R\bar{3}c$, no signals of impurities were detected.

Single crystals of compounds **I**–**III** were prepared 2–3 h after the addition of an excess of an alcoholic solution of nitrate of the same lanthanide(III) to the prepared violet solution containing the complex cation. The experimental data were collected on a Bruker SMART APEX II diffractometer at 150 K (MoK_α radiation, λ = 0.71073 Å, graphite monochromator) in the ω scan mode. The data were corrected for absorption by the measured intensities of equivalent reflections [5]. The structure was solved by a direct method and refined by the full-matrix anisotropic least-squares method with respect to F^2 for all non-hydrogen atoms [6]. Hydrogen atoms were placed in the calculated positions and refined according to the "rider" model. Selected crystal data, details of data collection, and the characteristics of refinement of structures **I**–**III** are listed in Table 1. Full tables of coordinates of atoms, bond lengths, and valence angles are deposited with the Cambridge Structural Database, CCDC nos. 1509658–1509660 for complexes **III**, **II**, and **I**, respectively (http://www.ccdc.cam.ac.uk).

X-ray powder diffraction patterns of complexes **I**–**III** were obtained on a Bruker D8 Advance diffractometer (CuK_α radiation, λ = 1.5418 Å, Ni-filter, LYNXEYE detector, reflection geometry). The measurements were made in the range of 2θ angles of 5°–60°. The STOE WinXPOW software package was used for processing X-ray diffraction patterns (removal of $K_{\alpha 2}$ lines, profile analysis, and indication and refinement of unit cell parameters) using. Theoretical X-ray diffraction patterns for **I**–**III** were calculated in the Mercury program based on the obtained X-ray diffraction data.

The electronic absorption spectra were measured on a SF2000 spectrophotometer in quartz cells (1 cm). The spectra were decomposed into Gaussian components to clarify the position of the absorption maxima and determine accurately the molar absorption coefficients. The obtained data were interpreted in terms of

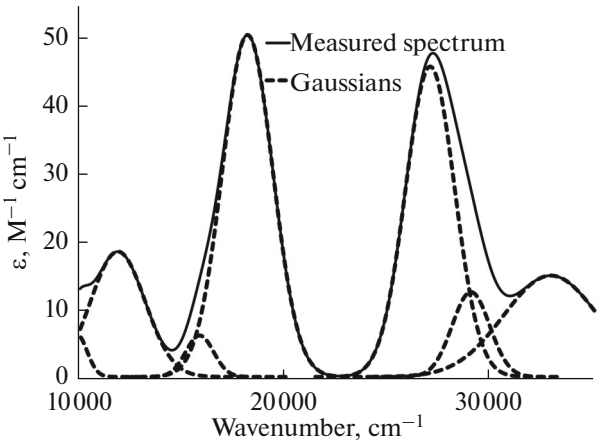

Fig. 1. Representative measured electronic absorption spectrum of complexes **I**–**III** (ethanol, 25°C) expanded to Gaussian components.

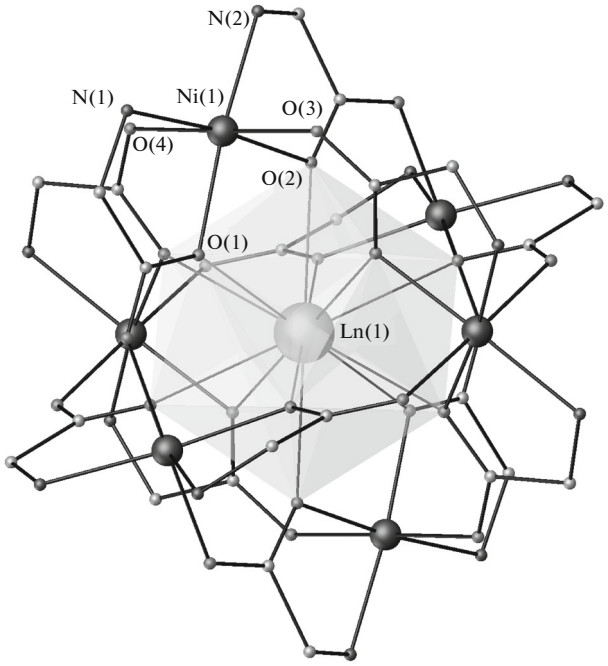

Fig. 2. Molecular structure of complex cation $[Ln\{Ni(Gly)_2\}_6]^{3+}$ in complexes **I**–**III** (Ln = La, Ce, and Pr; Gly-glycinate; hydrogen atoms are not shown).

the ligand field theory (the symmetry of the environment of the Ni(II) ion to be C_{2v}).

The complex cation in the alcoholic solution was also tried to be prepared using the reaction of nickel(II) glycinate with lanthanum nitrate. Due to the low solubility of glycinate in alcohol, the process was carried out on heating (60°C). When the mixture was heated for a long time, the solution over the solid nickel(II) glycinate turned to be pale-violet, but no noticeable dissolution of the precipitate was observed. Instead, the original blue precipitate gradually turned purple. Apparently, the cation–anion complex **I** has low solubility in ethanol, and in the presence of excess lanthanum nitrate in the solution above the precipitate is released into the solid phase. A similar situation was observed for cerium and praseodymium. In the case of neodymium nitrate, the violet color of the solution (or a change in the color of the precipitate to violet) was not observed under these conditions.

RESULTS AND DISCUSSION

A characteristic feature of the formation of complex cation $[Ln\{Ni(Gly)_2\}_6]^{3+}$ is a change in color from green (nickel(II) aqua complex) or blue (nickel(II) glycinate) to violet. A detailed analysis of the electronic absorption spectra of solutions of the complex cation (with the expansion of bands into Gaussian components and using data on similar nickel(II) complexes [7]) showed that the bands in the visible region correspond to exclusively *d*–*d* electronic transitions. Long-wave bands in the spectra (>30000 cm^{-1}, Fig. 1) were attributed to the transitions between the corresponding terms (Table 2). Thus, the color change during the synthesis of $[Ln\{Ni(Gly)_2\}_6]^{3+}$ in the solution is caused by a rearrangement of the coordination environment of the nickel(II) ion to form neutral supramolecular fragment $\{Ni(Gly)_2\}_6$.

Crystals of complexes **I**–**III** are isostructural. The unit cell parameters of **I**–**III** have no dependence on the nature of the lanthanide(III) central ion (Table 1).

An interesting feature is observed in the molecular structure of complex cation $[Ln\{Ni(Gly)_2\}_6]^{3+}$ (Ln = La, Ce, and Pr) (Fig. 2). The Ln(III) ion is located in

Table 2. Assignment of absorption bands in the electronic spectra of complexes **I**–**III**

Gaussian	1	2	3	4	5	6
Energy*, cm^{-1}	29100	26800	18300	15500	12100	9950
ε*, l/mol/cm	10	45	50	5	20	5
Excited state	$^3T_{2g}(A_1)$	$^3T_{2g}(A_2)$	$^3T_{1g}(B_2)$	$^3T_{1g}(B_1)$	$^3T_{1g}(B_2)$	$^3T_{1g}(B_1)$

* Standard deviation: ±10 cm^{-1} for wavenumber; ±20% for ε. The ground state for all electronic transitions is $^3B_1$.

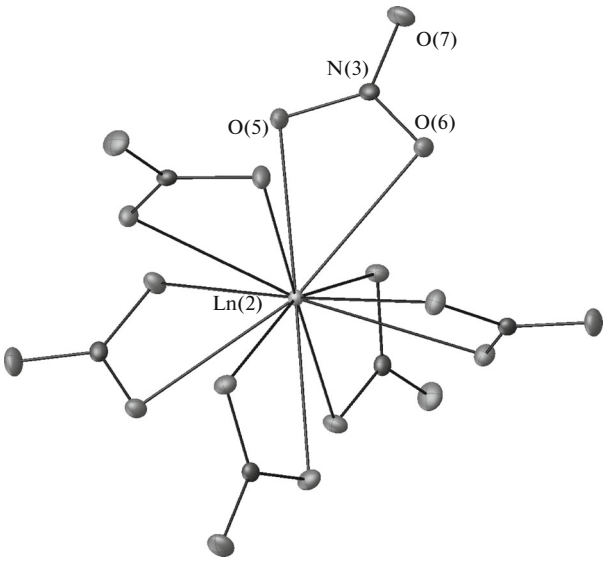

Fig. 3. Molecular structure of complex anion $[Ln(NO_3)_6]^{3-}$ in complexes **I**–**III** (Ln = La, Ce, and Pr; ellipsoids of thermal oscillations are given with the 50% probability level).

Table 3. Selected interatomic distances (*d*) and angles (ω) in the structures of **I**–**III**

Compound	I	II	III
Bond; angle	*d*, Å; ω, deg	Bond; angle	*d*, Å; ω, deg
Cation			
Ln1–O1	2.7166(12)	2.7153(15)	2.7109(15)
Ln1–O2	2.6993(12)	2.6901(15)	2.6867(14)
O1–Ln1–O2	64.38(3)	64.30(4)	64.28(4)
Ni1–O1	2.039(2)	2.042(6)	2.044(6)
Ni1–O2	2.048(2)	2.048(5)	2.046(7)
Ni1–O3	2.053(3)	2.050(7)	2.047(5)
Ni1–O4	2.054(3)	2.056(7)	2.050(7)
Ni1–N1	2.062(3)	2.057(8)	2.056(7)
Ni1–N2	2.066(3)	2.076(7)	2.073(7)
O1Ni1N1	83.04(5)	83.16(7)	83.34(6)
O2Ni1N2	81.98(5)	82.21(7)	82.34(7)
O1Ni1O2	92.10(5)	91.78(6)	91.46(6)
N1Ni1N2	102.92(6)	102.91(8)	102.92(7)
O1Ni1O3	91.40(5)	91.42(6)	91.45(6)
O2Ni1O4	89.52(5)	89.71(6)	89.72(6)
O1Ni1O4	90.03(5)	89.49(6)	89.76(6)
O2Ni1O3	89.65(5)	89.85(6)	89.51(6)
Anion			
Ln2–O5	2.6255(13)	2.6033(18)	2.5914(17)
Ln2–O6	2.6643(13)	2.6522(16)	2.6395(16)
O5Ln2O6	48.87(8)	49.1(2)	49.4(2)

an almost ideal icosahedral environment of the oxygen atoms of the $\{Ni(Gly)_2\}_6$ fragment. However, paradoxically, the central ion has no effect on the size of this icosahedral cavity. As the ionic radius of Ln^{3+} decreases, the size of the cavity (determined by the distances between the oxygen atoms lying opposite each other in the icosahedron) remains unchanged within the measurement error (Table 3). This means that the $\{Ni(Gly)_2\}_6$ fragment formed by six slightly distorted NiN_2O_4 octahedra has an exceptional rigidity.

In anion $[Ln(NO_3)_6]^{3-}$ (Ln = La, Ce, and Pr), the central ion is surrounded by six bidentate nitrate anions (Fig. 3). The Ln–O interatomic distances are in agreement with those for analogous complex anions, according to the Cambridge Structural Database. At the same time, the Ln–O distances naturally decrease from lanthanum to praseodymium (i.e., the size of the anion decreases) demonstrating the flexibility of the Ln(III) coordination environment in the anion, unlike that in the complex cation.

In the crystal, complex cations and anions are joined together by weak hydrogen bonds N–H···O (d(N–H) = 0.91, d(H···O) = 2.26, d(N···O) = 3.146(3) Å; angle N–H···O = 164.4°), forming a dense packing in which there are no molecules of any solvents (Fig. 4).

The rigidity of the supramolecular fragment $\{Ni(Gly)_2\}_6$ surrounding the central lanthanide ion can affect the stability of such a complex cation over the lanthanide series. The stability of the complex should change monotonically in accordance with the change in the Ln^{3+} ionic radius. Since the interaction between Ln(III) and oxygen atoms is predominantly ionic, we can expect a decrease in the stability of the complex cation; therefore, this complex may be unstable starting with some lanthanide. Unfortunately, the precise determination of the stability limit of the complex cation over the lanthanide series is complicated by the fact that, along with the reaction for obtaining the desired product, side processes can occur simultaneously, among which the hydrolysis of the Ln(III) ion (amplified from La to Lu) has the greatest effect [8]. Therefore, the results of this work cannot help to answer unambiguously to the question of existence of a complex cation of neodymium similar to those found for lanthanum, cerium, and praseodymium solved by. Additional studies are needed, possibly with the replacement of the solvent in the synthesis of *d*- and *f*-metal precursors.

ACKNOWLEDGMENTS

This work was supported by the Russian Foundation for Basic Research, project no. 16-33-00604 mol_a.

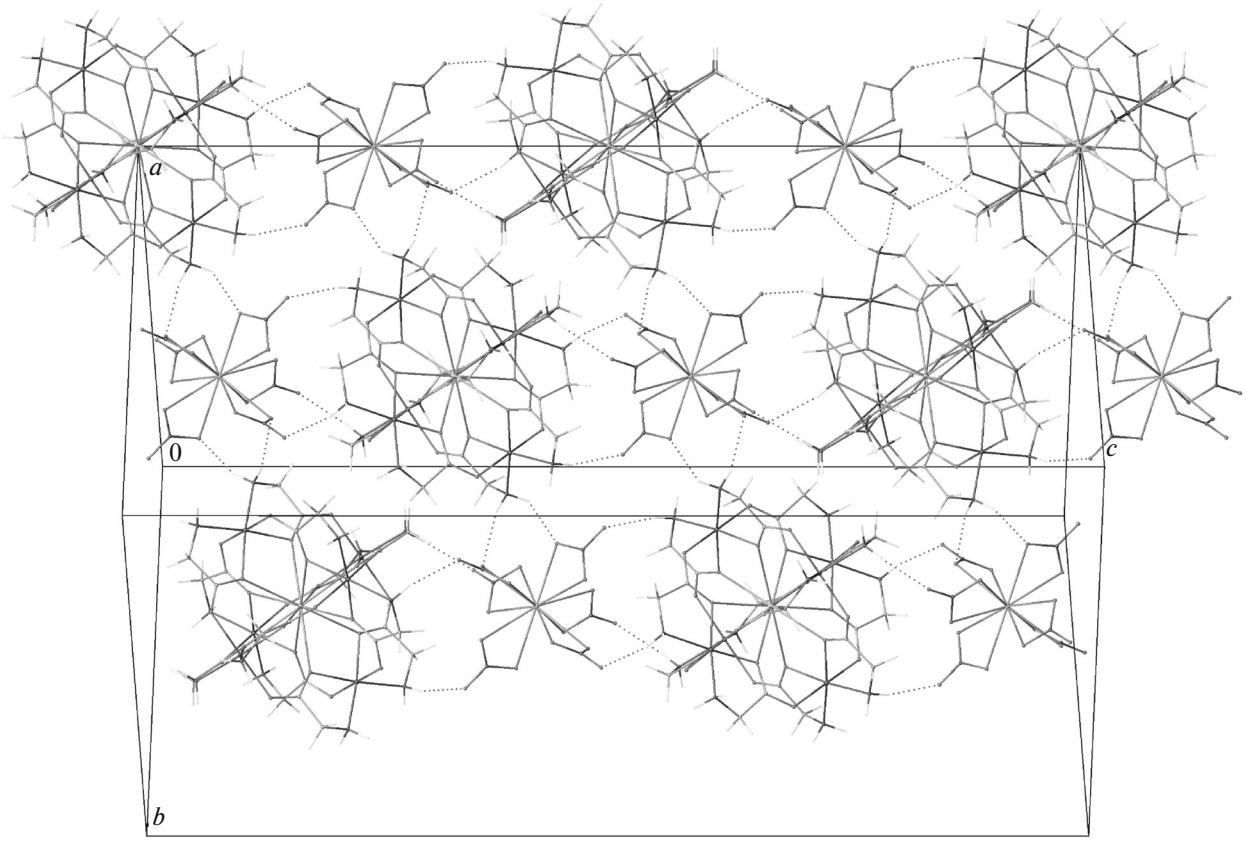

Fig. 4. Packing of complex cations and anions in crystals of complexes **I**–**III**.

REFERENCES

1. K. Liu, W. Shi, and P. Cheng, Coord. Chem. Rev. **289**, 74 (2015). 2015.
2. G. J. Sopasis, A. B. Canaj, C. J. Milios, et al., Inorg. Chem. **51**, 5911 (2012).
3. S. I. Bezzubov, V. D. Doljenko, Yu. M. Kiselev, et al., Acta Crystallogr., Sect. E **71**, m183 (2015).
4. T. Yasui, Bull. Chem. Soc. Jpn. **38**, 1746 (1965).
5. G. M. Sheldrick, SADABS: Program for Scaling and Correction of Area Detector Data (Univ. of Göttingen Göttingen, 1997).
6. G. M. Sheldrick, Acta Crystallogr., Sect. A **64**, 112 (2008).
7. P. L. Meredith and R. A. Palmer, Inorg. Chem. **10**, 1049 (1971).
8. J.-J. Zhang, S.-M. Hu, S.-C. Xiang, et al., Polyhedron **25**, 1 (2006).

Translated by V. Avdeeva